

ChemComm

Chemical Communications

Accepted Manuscript



This is an Accepted Manuscript, which has been through the Royal Society of Chemistry peer review process and has been accepted for publication.

Accepted Manuscripts are published online shortly after acceptance, before technical editing, formatting and proof reading. Using this free service, authors can make their results available to the community, in citable form, before we publish the edited article. We will replace this Accepted Manuscript with the edited and formatted Advance Article as soon as it is available.

You can find more information about Accepted Manuscripts in the [Information for Authors](#).

Please note that technical editing may introduce minor changes to the text and/or graphics, which may alter content. The journal's standard [Terms & Conditions](#) and the [Ethical guidelines](#) still apply. In no event shall the Royal Society of Chemistry be held responsible for any errors or omissions in this Accepted Manuscript or any consequences arising from the use of any information it contains.

COMMUNICATION

Efficient biocatalytic C-H bond oxidation: an engineered heme-thiolate peroxygenase from a thermostable cytochrome P450

Received 00th January 20xx,
Accepted 00th January 20xxAlecia R. Gee,^a Isobella S. J. Stone,^a Tegan P. Stockdale,^b Tara, L. Pukala,^a James J. De Voss,^b and Stephen G. Bell^{*a}

DOI: 10.1039/x0xx00000x

A highly sought after reaction in chemical synthesis is the activation of unactivated carbon-hydrogen bonds. We demonstrate the hydroxylation of fatty acids using an engineered thermostable archaeal cytochrome P450 enzyme. By replacing a seven amino acid section of the I-helix, the nicotinamide cofactor-dependent monooxygenase was converted into a hydrogen peroxide using peroxygenase, enabling the efficient biocatalytic oxidation of C-H bonds at room temperature to 90 °C.

The enzymes of the cytochrome P450 superfamily are important biocatalysts due to their ability to selectively catalyse C–H bond oxidation on a broad range of substrates.^{1–4} Typically, these heme enzymes depend on expensive nicotinamide cofactors and electron transfer partners to supply electrons to enable the heme to activate dioxygen (O₂) which generates the reactive intermediate (Compound I) required to oxidise their substrates (Scheme 1).⁵ The majority of these enzymes use an acid-alcohol pair within the I-helix to interact with the heme-oxygen intermediates and control the delivery of protons to them. These are essential steps within the normal catalytic cycle (Fig. 1 and Scheme 1).^{6, 7} Recently, a new family of cytochrome P450s – the CYP255A family – was characterised, whose members catalyse aromatic *O*-demethylation reactions.^{8, 9} This family of P450 enzymes does not depend on O₂ as an oxidant and does not have the conserved acid-alcohol pair; instead, these are replaced with a glutamine-glutamate pair of residues (Fig. 1). This change confers *peroxygenase* activity onto these heme enzymes allowing the use of H₂O₂ to drive their catalytic reactions.¹⁰ Interestingly, it has also been demonstrated previously that mutation of the conserved threonine of the acid-alcohol pair to glutamic acid can confer peroxygenase activity to P450 enzymes, with varying levels of effectiveness.^{11, 12}

Here we report the development of a new cytochrome P450 peroxygenase catalyst from the thermostable CYP119 enzyme found in the hyperthermophilic archaeum *Sulfolobus acidocaldarius*.^{13–17} This is a highly thermostable P450 enzyme

formed are negligible with all tested redox partners to date. It is therefore an ideal P450 enzyme to target in order to remove the redox partner liability and unleash its catalytic potential using peroxygenase activity. We demonstrate that, by replacing a seven amino acid section of this enzyme with that of a heme peroxygenase, the efficient oxidation of fatty acids using H₂O₂ at temperatures up to 90 °C is made possible.

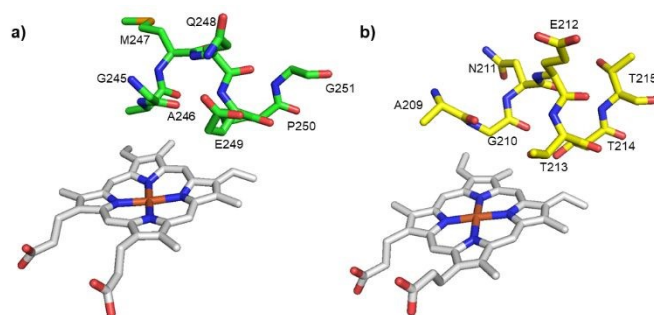
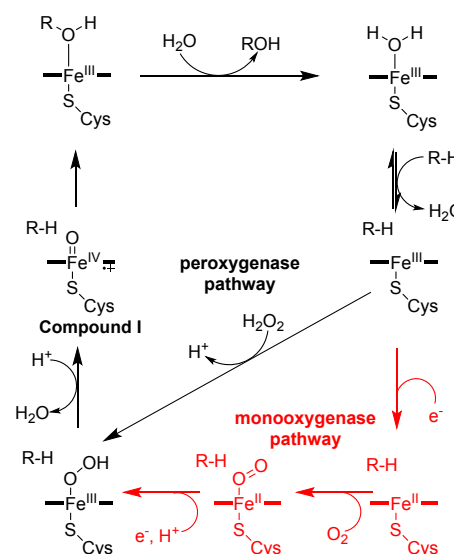


Fig. 1 The oxygen binding groove region of the I-helix in the active site of (A) CYP255A2 and (B) CYP119A1 is shown. The key residues surrounding the groove are GAMQEPG and AGNETTT for CYP255 and CYP119 respectively. The highly conserved acid alcohol pair within this groove in CYP119 (E212 and T213) is a glutamine-glutamate pair (Q248 and E249) for CYP255A2.



Scheme 1. The catalytic cycle of P450 monooxygenases. The peroxygenase pathway, which is highlighted in black, enables the enzyme to bypass the electron transfer steps and requirements for electron transfer partners in the monooxygenase pathway (additional steps in red).

^a School of Physics, Chemistry and Earth Sciences, University of Adelaide, Adelaide, SA 5005, Australia. E-mail: stephen.bell@adelaide.edu.au

^b School of Chemistry and Molecular Biosciences, University of Queensland, Brisbane, Qld, 4072, Australia

†Electronic Supplementary Information (ESI) available: See DOI: 10.1039/x0xx00000x

and is known to oxidise fatty acids but the levels of product

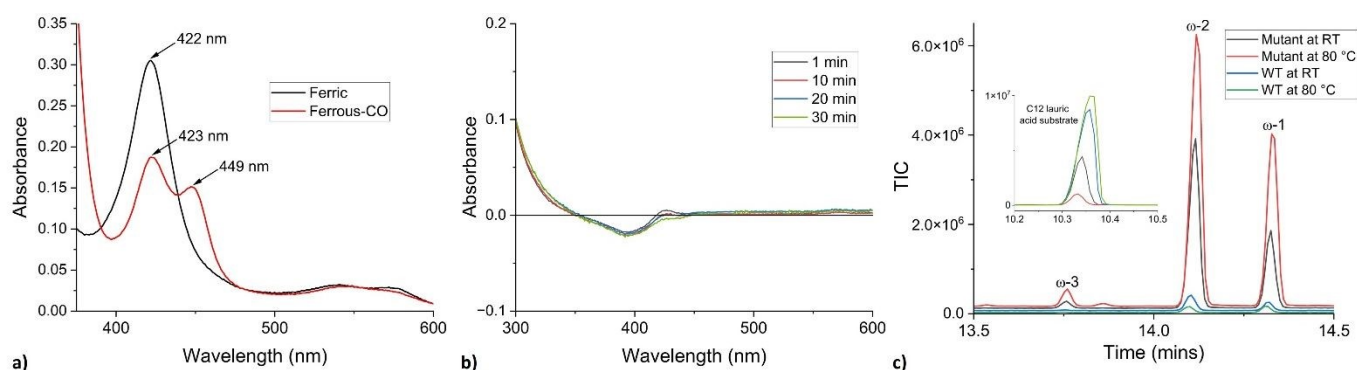


Fig. 2 (a) The UV-vis absorbance spectra of the ferric (black) and ferrous-CO bound (red) iron centre in the CYP119 GALQEPG peroxygenase mutant (CYP119-perox7). (b) Heme bleaching assay of CYP119-perox7 (3 μ M, Absorbance maxima \sim 0.31 absorbance units) in the presence of substrate dodecanoic acid (1 mM) and hydrogen peroxide (60 mM). Low levels of heme degradation are observed over 30 minutes; see ESI for further details (Fig. S4-S7). (c) Gas chromatogram (GC-MS) of the oxidation of dodecanoic acid by wild type (WT) CYP119A1 and CYP119-perox7 (mutant) at room temperature (RT) and 80 $^{\circ}$ C using hydrogen peroxide (60 mM).

Codon optimised genes encoding the wild-type (WT) and a mutant CYP119 enzyme, were obtained in a pET vector (see SI for details). The mutant (CYP119-perox7) was designed to replace the seven amino acid residues of the I-helix of WT CYP119 with the equivalent residues found in the CYP255 family, with the exception of the easily oxidised methionine residue, which was substituted with a leucine. Overall, the seven amino acids of CYP119²⁰⁹AGNETTT²¹⁵ were replaced with the sequence GALQEPG. The His-tagged proteins were produced in *E. coli* and purified using affinity and anion exchange chromatography (see SI for details). UV-vis spectroscopic characterisation of the WT and the mutant CYP119 enzymes were conducted to compare their properties. The UV-vis spectra of the ferric (substrate-free and dodecanoic acid-bound), and ferrous-CO forms of WT CYP119 were typical for cytochrome P450 enzymes (Fig. S1-3, Soret maximum at $A_{415\text{ nm}}$). A calculated extinction coefficient of WT CYP119, $\epsilon_{415\text{ nm}} = 121\text{ mM}^{-1}\text{cm}^{-1}$, was used for enzyme concentration quantitation.¹⁶ Ferric CYP119-perox7 had a Soret absorbance maximum at 422 nm and the heme α - and β -bands also shifted to slightly longer wavelengths (Fig. 2a). Upon binding of dodecanoic acid, a blue shift is observed, resulting in a Soret peak of 420 nm (Fig. S2, see ESI for WT data). Unlike the WT enzyme full conversion of the Soret band to 449 nm was not observed in the ferrous CO-bound spectrum (Fig. 2 and Fig. S3).

Addition of H_2O_2 to P450 enzymes can result in destruction of the heme cofactor, leaving the enzyme inactive.¹⁸ Heme bleaching assays were used to assess the stability of the CYP119 to the presence of H_2O_2 . The destruction of heme was monitored by the change in UV-vis absorbance of the Soret peak of CYP119. In the presence of dodecanoic acid the addition of 60 mM peroxide resulted in very little change in the UV-vis absorbance spectrum of CYP119-perox7 over a period of 30 minutes (Fig. 2b and Fig. S4-S7). This was more stable than the WT enzyme (Fig. S4-S7) and demonstrates that the new biocatalyst is resistant to heme destruction by H_2O_2 in the presence of a suitable substrate.^{18, 19}

Gas Chromatography-Mass Spectrometry (GC-MS) analysis of BSTFA/TMSCl derivatised H_2O_2 -driven reactions was used to identify the metabolites of dodecanoic acid oxidation. Room temperature reactions in which 50 mM H_2O_2 was added to the

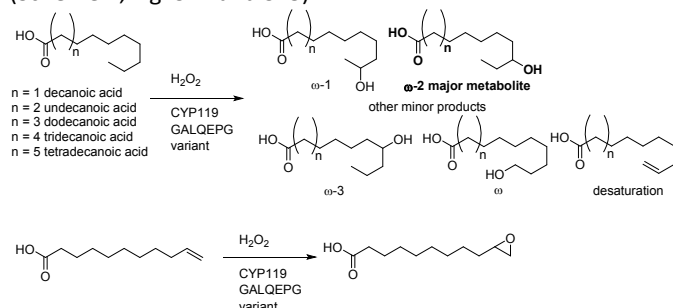
substrate-bound enzyme (3 μ M enzyme and 1 mM dodecanoic acid) were analysed over 2 hours. The analysis of the reactions with WT CYP119 showed the formation of low levels of products. In contrast CYP119-perox7 converted the substrate into a mixture of metabolites with a greater than 10-fold improvement over the WT enzyme at the same temperature. These were identified as arising from hydroxylation at predominantly the ω -2 (65.3%) and ω -1 (26.3%) positions with minor metabolites arising from oxidation at the ω and ω -3 positions and a low level of a metabolite from a desaturation reaction (Table 1, Scheme 2, Fig. S8 – S10). The major hydroxylated fatty acid metabolites formed during the P450 mediated oxidation reactions were also partially further oxidised to ketone metabolites (Table 1).

Table 1. Product distribution for fatty acid oxidation by the GALQEPG CYP119 peroxygenase. Standard deviations are provided in the SI (Table S1 and S2). The approximate relative yield of metabolites relative to C_{12} is also provided.

Metabolite	Fatty acid substrate					
	C10	C11	C12	C13	C14	C12d ₄
Relative turnover	10	80	100	100	10	-
desaturation	6.2	1.7	0.3	0.3	-	-
ω C(O-H)	4.1	0.5	0.4	0.2	-	0.7
ω -1 C(O-H)	73.2	76.6	26.3	44.5	31.5	63.1
ω -2 C(O-H)	16.5	16.4	65.3	33.6	59.0	26.7
ω -3 C(O-H)	-	0.6	2.7	18.1	6.7	0.7
ω -4 C(O-H)	-	-	-	0.9	2.9	-
ω -1 C=O	-	3.4	1.2	1.1	-	6.6
ω -2 C=O	-	0.9	3.8	0.9	-	2.1
ω -3 C=O	-	-	-	0.3	-	-

The selectivity of the WT enzyme was similar to the mutant (Fig. 2c) though analysis of the minor products was difficult due to their low level of formation. Minor differences in selectivity compared to previous reports using other oxygen donors can be ascribed to the known changes in the product distribution of CYP119 at different pH values (Table 1 and Table S1).^{20, 21}

Similar reactions were repeated using the conditions from above for fatty acids ranging from C₁₀ to C₁₄ in length to determine the optimal substrate and the variations in the product distribution as the length of the carbon chain increased (Fig. S11-S21). Reactions with 10-undecenoic acid were also undertaken over 4 hrs to determine the effect of adding a terminal alkene moiety on the reaction chemoselectivity (Scheme 2, Fig. S12 and S13).



Scheme 2. The metabolites generated from the oxidation of fatty acids and 10-undecenoic acid by the GALQEPG variant of CYP119.

Dodecanoic and tridecanoic acid were the best substrates in terms of conversion, with activity dropping off dramatically for the shorter (decanoic acid) and longer (tetradecanoic acid) fatty acids (Table 1). The regiochemistry of oxidation of these substrates by CYP119-perox7 was in broad agreement with that observed for dodecanoic acid; the major sites of oxidation were toward the ω end of the chain (Table 1). However, changes in the location of C-H bond abstraction occurred as the chain length varied. For longer fatty acids, including tetradecanoic acid, the product distribution moved away from the terminal position and some oxidation was observed at ω-4. For the odd numbered carbon chain of tridecanoic acid, there was a switch in preference for oxidation at ω-2 to ω-1 as well as an increase in the amount of the ω-3 metabolite (Figure S11 and Table 1). The oxidation of the shorter decanoic acid and undecanoic acid by CYP119-perox7 resulted in a switch in the oxidation selectivity to the ω-1 carbon over ω-2. Undecanoic acid oxidation generated more product than 10-undecenoic acid (approx. 3-fold increase) but the oxidation of the latter was more selective generating predominantly a single major metabolite (98%; Figure S12). This was identified as the epoxide

(Scheme 2) by synthesis of the standard and GC-MS analysis (Figure S12-S13; see SI for further details). This is in agreement with what has been reported previously with the WT enzyme.²²

Having established that dodecanoic acid is a preferred substrate for CYP119-perox7 we used this to further optimise and assess the activity of the peroxygenase enzyme. We explored the effect of temperature on the peroxygenase activity. Raising the temperature increased the activity of the enzyme with greater substrate conversion being observed at 50 °C as well as at 70 °C, 80 °C and 90 °C compared to RT (Fig. 2c and 3a). The product distribution was broadly similar at the higher temperatures though there was a slight decrease in regioselectivity, with an increase in ω and ω-1 oxidation observed at the expense of ω-2 reaction (Table 2). At 80 °C the mutant generated >35-fold more oxidised metabolites than the best activity with the WT enzyme (Fig. 2c). This is important as it demonstrates that not only is the thermostability of the engineered enzyme maintained but that it is highly active at temperatures which are not usually available for enzyme catalysed hydroxylation reaction of C-H bonds.

Previously we and others have used the deuterated substrate [9,9,10,10-*d*₄]-dodecanoic acid to monitor the intrinsic kinetic isotope effect of C-H bond activation in P450 catalysed reactions by assessing changes in the product distribution compared to dodecanoic acid. Comparative oxidation reactions were performed with deuterated and non-deuterated dodecanoic acid with the CYP119-perox7 variant (Fig. 3b, Fig S22 and S23).²³

Table 2. Product distribution for dodecanoic acid oxidation by the CYP119-perox7 mutant at different temperatures. A more detailed analysis of the distribution including further oxidation metabolites are provided in the ESI (Table S3).

metabolite	temperature				
	RT	50 °C	70 °C	80 °C	90 °C
ω C	0.5	0.2	0.6	0.9	0.8
ω-1	26.9	21.9	29.2	34.4	34.7
ω-2	63.7	45.8	50.3	55.6	56.7
ω-3	2.3	2.1	2.7	3.0	2.9

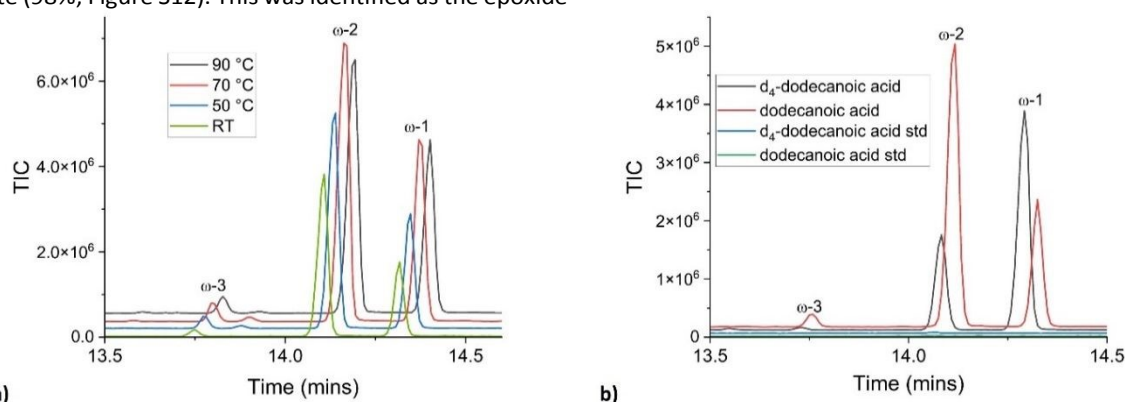


Fig. 3 (a) GC-MS analysis of the oxidation of dodecanoic acid (1 mM) by CYP119-perox7 (3 μM) at room temperature (RT) and 50 °C, 70 °C and 90 °C using hydrogen peroxide (60 mM). (b) Gas chromatography analysis of the oxidation of dodecanoic (lauric) acid and [9,9,10,10-*d*₄]-dodecanoic acid by CYP119-perox7 at room temperature (RT) using hydrogen peroxide.

There was a significant decrease in the levels of hydroxylated fatty acids at the deuterated ω -2 and ω -3 positions (Figure 3b and Table 1) and an increase in the ω -1 metabolite. The changes in the product distributions enabled an intrinsic kinetic isotope effect (KIE) of 6.4 ± 0.3 to be calculated (Table S2). These results are similar to those reported previously for WT CYP119 and d_4 -dodecanoic acid turnovers supported with *m*-chloroperbenzoic acid (KIE 6.6)²³ and those observed with other P450 enzymes.²⁴ This demonstrates that C–H bond abstraction is kinetically important in the peroxygenase mechanism, consistent with the radical rebound mechanism proposed for typical P450 monooxygenases that proceed via Cpd I. The rate of dodecanoic and tetradecanoic acid oxidation by CYP119-perox7 at 70 °C were 19.6 ± 1.0 and $17.9 \pm 1.5 \text{ min}^{-1}$, respectively (Fig. S24 and Fig. S25). The rate of oxidation of tetradecanoic acid at 30 °C was $5.4 \pm 1.7 \text{ min}^{-1}$. The rates at 70 °C are more than double those obtained previously with the T213E single mutant under similar conditions.¹²

In summary, we have engineered increased peroxygenase activity into the thermostable cytochrome P450 enzyme CYP119 by replacing a seven amino acid portion of the I-helix with that from a dual function P450 peroxygenase/monooxygenase enzyme. This new peroxygenase mutant was stable to hydrogen peroxide in the presence of substrate and capable of hydroxylating fatty acid substrates with high levels of substrate conversion (>99%) and good turnover numbers (>330). These are >35-fold more than the WT enzyme.^{12,25} with significant scope for further optimisation. The thermostability of the enzyme was maintained and catalytic activity at high temperatures, 50 °C to 90 °C, was demonstrated. This achieves a long sought after goal of effectively reconstituting the activity of a highly thermostable heme-dependent oxygenase enzyme using a single, cheap, and clean cooxidant/cofactor. The generation of an efficient thermostable heme peroxygenase establishes a system which overcomes many of the major drawbacks associated with using heme enzymes for selective C–H bond hydroxylation. These include the requirement for expensive nicotinamide cofactors and electron transfer partners, and the low activity and stability of enzymes. It also provides a new stable enzyme scaffold for enzymatic C–H activation. Further biochemical study and reaction engineering to optimise the activity and structural and protein engineering investigations to expand the substrate range and reaction scope of CYP119 will enable the design of bespoke biocatalysts for selective oxidation reactions.

This work was funded, in part, through Australian Research Council grant DP200102411 (to SGB and others). ARG was supported by a Research Training Program (RTP) scholarship from the Australian government and thanks CSIRO Advanced Engineering Biology Future Science Platform (AEB FSP) for a top-up Scholarship.

Conflicts of interest

The University of Adelaide have filed a provisional patent related to this research.

References

1. A. Greule, J. E. Stok, J. J. De Voss and M. J. Cryle, *Nat Prod Rep*, 2018, **35**, 757-791.
2. E. Romero, B. S. Jones, B. N. Hogg, A. Rué Casamajo, M. A. Hayes, S. L. Flitsch, N. J. Turner and C. Schnepel, *Angew Chem Int Ed Engl*, 2021, **60**, 16824-16855.
3. Z. Li, Y. Jiang, F. P. Guengerich, L. Ma, S. Li and W. Zhang, *J Biol Chem*, 2020, **295**, 833-849.
4. S. Chakrabarty, Y. Wang, J. C. Perkins and A. R. H. Narayan, *Chem Soc Rev*, 2020, **49**, 8137-8155.
5. D. Holtmann, M. W. Fraaije, I. W. C. E. Arends, D. J. Opperman and F. Hollmann, *Chem Commun*, 2014, **50**, 13180-13200.
6. S. Nagano and T. L. Poulos, *J Biol Chem*, 2005, **280**, 31659-31663.
7. T. Coleman, J. E. Stok, M. N. Podgorski, J. B. Bruning, J. J. De Voss and S. G. Bell, *J. Biol. Inorg. Chem.*, 2020, **25**, 583-596.
8. S. J. B. Mallinson, M. M. Machovina, R. L. Silveira, M. Garcia-Borrás, N. Gallup, C. W. Johnson, M. D. Allen, M. S. Skaf, M. F. Crowley, E. L. Neidle, K. N. Houk, G. T. Beckham, J. L. DuBois and J. E. McGeehan, *Nature Commun*, 2018, **9**, 2487-2487.
9. M. M. Fetherolf, D. J. Levy-Booth, L. E. Navas, J. Liu, J. C. Grigg, A. Wilson, R. Katurah, G. T. Beckham, W. W. John and L. D. Eltis, *Proc Nat Acad Sci - USA*, 2020, **117**, 25771-25778.
10. A. C. Harlington, K. E. Shearwin, S. G. Bell and F. Whelan, *Chem Commun*, 2022, **58**, 13321-13324.
11. M. N. Podgorski, J. S. Harbort, J. H. Z. Lee, G. T. H. Nguyen, J. B. Bruning, W. A. Donald, P. V. Bernhardt, J. R. Harmer and S. G. Bell, *ACS Catal*, 2022, **12**, 1614-1625.
12. O. Shoji, T. Fujishiro, K. Nishio, Y. Kano, H. Kimoto, S.-C. Chien, H. Onoda, A. Muramatsu, S. Tanaka, A. Hori, H. Sugimoto, Y. Shiro and Y. Watanabe, *Catal Sci Technol*, 2016, **6**, 5806-5811.
13. K. S. Rabe, K. Kiko and C. M. Niemeyer, *Chembiochem*, 2008, **9**, 420-425.
14. C. R. Nishida and P. R. Ortiz de Montellano, *Biochem Biophys Res Commun*, 2005, **338**, 437-445.
15. J. K. Yano, L. S. Koo, D. J. Schuller, H. Li, P. R. Ortiz de Montellano and T. L. Poulos, *J Biol Chem*, 2000, **275**, 31086-31092.
16. M. A. McLean, S. A. Maves, K. E. Weiss, S. Krepich and S. G. Sligar, *Biochem Biophys Res Commun*, 1998, **252**, 166-172.
17. R. L. Wright, K. Harris, B. Solow, R. H. White and P. J. Kennelly, *FEBS Lett*, 1996, **384**, 235-239.
18. P. C. Cirino and F. H. Arnold, *Angew Chem Int Ed*, 2003, **42**, 3299-3301.
19. A. Greule, T. Izoré, D. Machell, M. H. Hansen, M. Schoppet, J. J. De Voss, L. K. Charkoudian, R. B. Schittenhelm, J. R. Harmer and M. J. Cryle, *Front Chem*, 2022, **10**, 868240.
20. Z. Su, J. H. Horner and M. Newcomb, *Chembiochem*, 2012, **13**, 2061-2064.
21. L. S. Koo, C. E. Immoos, M. S. Cohen, P. J. Farmer and P. R. Ortiz de Montellano, *J Am Chem Soc*, 2002, **124**, 5684-5691.
22. X. Chen, Z. Su, J. H. Horner and M. Newcomb, *Org Biomol Chem*, 2011, **9**, 7427-7433.
23. Z. Su, J. H. Horner and M. Newcomb, *Chemistry*, 2019, **25**, 14015-14020.
24. J. Akter, T. P. Stockdale, S. A. Child, J. H. Z. Lee, J. J. De Voss and S. G. Bell, *J Inorg Biochem*, 2023, **244**, 112209.
25. E. K. Doğru, G. Güralp, A. Uyar, N. B. Surmeli, *J Mol Graph Model*, 2023, **118**, 108323